REPRODUCTION
RESEARCH

Tracking the rejection and survival of mouse ovarian iso- and allografts *in vivo* with bioluminescent imaging

Chi-Huang Chen[1,2], Yu-Chi Yeh[3,4], Gwo-Jang Wu[2], Yen-Hua Huang[5], Wen-Fu Thomas Lai[1], Jah-Yao Liu[2] and Chii-Ruey Tzeng[1,4,6]

[1]Graduate Institute of Clinical Medicine, Taipei Medical University, Taipei 110, Taiwan, ROC, [2]Departments of Obstetrics and Gynecology, Tri-Service General Hospital, National Defense Medical Center, Taipei 114, Taiwan, ROC, [3]Department of Psychiatry, Cathay General Hospital, Taipei 106, Taiwan, ROC, [4]School of Medicine and [5]Department of Biochemistry and Graduate Institute of Medical Sciences, Taipei Medical University, Taipei 110, Taiwan, ROC and [6]Center for Reproductive Medicine and Sciences, Taipei Medical University and Hospital, Taipei, Taiwan, ROC

Correspondence should be addressed to C-R Tzeng who is now at College of Medicine, Taipei Medical University, No. 250, Wusing Street, Sinyi District, Taipei City 110, Taiwan, ROC; Email: tzengcr@tmu.edu.tw

Abstract

The applications of *in vivo* bioluminescent imaging (BLI) with a luciferase reporter gene occur widely across biomedical fields. Luciferase-transgenic mice are highly useful donors for tracking transplanted ovarian tissues. Realizing the full potential of this system may greatly benefit the study of the physiological behaviour and function of transplanted grafts, and the rapid and reliable evaluation of new transplantation protocols. The ovarian tissues of donor FVB/N-Tg(*PolII–Luc*)Ltc transgenic mice, with a luciferase transgene as the reporter, were transplanted into iso/allogeneic recipients. Rejection, ovarian function and BLI were quantitatively analysed *in vivo* over time. The BLI of the ovarian isografts revealed longer survival than that of allografts, even with cyclosporine A (CsA) treatment. The $CD4^+/CD8^+$ ratios of peripheral T-cells were significantly reduced in allografts compared with those in isografts ($P<0.0001$) during rejection, whereas $CD19^+$ cell numbers were higher in allografts. The infiltration of $CD4^+/CD8^+$ cells into the graft was unremarkable in isografts from day 1, but was strong in allografts from day 8 onwards. Hormone activity revealed complete oestrus cycles in the isografts but only the dioestrus stage in the allografts. These results demonstrate that BLI *in vivo* expedites the fast throughput and fate maps of ovarian grafts. The use of BLI to longitudinally monitor ovarian grafts for immunorejection demonstrated the short survival of allografts and the much longer survival of isografts. CsA treatment alone is ineffective against the acute rejection of ovarian allografts.

Reproduction (2010) **140** 105–112

Introduction

New discoveries applied to the preservation of fertility have created an unprecedented need for assisted reproductive technologies in young patients undergoing cancer therapy or with premature ovarian failure (POF; Donnez *et al*. 2006). In the past decade, much effort has been devoted to oocyte and ovary cryopreservation for autotransplantation (Kim *et al*. 2001, Chen *et al*. 2003, Kuwayama *et al*. 2005).

A series of discordant monozygotic twins restored fertility after ovarian isotransplantation from the fertile sister to their sibling who had POF, which offered a fascinating model beyond the mainstream of autotransplantation after ovarian cryopreservation (Silber *et al*. 2005, 2008, Silber & Gosden 2007). Extension of this technique and its application to ovarian homotransplantation (allografts) are probable developments in fertility preservation, because gamete and embryo donations are now mature and organized practices (Woodruff 1960; ASRM Practice Guidelines 2006, Guidelines for Gamete and Embryo Donation, http://www.asrm.org/detail.aspx?id=131).

Recent success has been reported with ovarian allografts in recipients who suffer from Turner's syndrome, because they can restore pubertal development (Mhatre *et al*. 2005). However, ovarian allografts are still relatively rare, and the processes of immune surveillance are unclear when immune privilege is absent (Gosden 2007). With the lack of extensive human and animal studies, the rejection immunity involved in ovarian allografts remains largely unexplored. Traditional transplant studies of rejection and immunity have been predominantly undertaken *in vitro* or *in vivo* with extensive, tailored sample collection in either animal or human models. With the advent of *in vivo* bioluminescent imaging (BLI), luciferase reporter genes have been used widely in various biomedical fields for the non-invasive investigation of the cellular molecular events involved in normal and pathological processes (Zinn *et al*. 2008).

ISSN 1470–1626 (paper) 1741–7899 (online)
DOI: 10.1530/REP-09-0448
Online version via www.reproduction-online.org

Luciferase-transgenic mice have been used as highly useful donors for monitoring hepatocyte, islet and stem cell transplantation (Yang *et al*. 2003, Fowler *et al*. 2005, Min *et al*. 2006). Realizing the full potential of this system may greatly benefit the study of the physiological behaviour and function of transplanted grafts.

Most cells infiltrating the allografts express T-cell markers, and are generally a mixture of $CD4^+$ and $CD8^+$ cells. The ratio of $CD4^+/CD8^+$ cells may vary in early versus late acute rejection (Hoshinaga *et al*. 1984, Ibrahim *et al*. 1993). CD19 is expressed earlier during B-cell development, and plays important roles in the peripheral immune system of diverse B-cell humoral transplant rejection (Yazawa *et al*. 2005).

We used optical molecular imaging, which expedites the fast-throughput screening of grafts, in a longitudinal study to monitor transplanted ovarian iso- and allografts in a comprehensive pilot model.

Results

The BLI photon quantity declined significantly below baseline in groups C and D from day 9 after transplantation, with no significant cyclic fluctuation. The most significant decline occurred in group C, all the way down to day 15. When the patterns of groups A and B were compared, there was a cyclic fluctuation every 4 days, but they were deeper in group A and only slight in group B, which presented the oestrus cycle as mild graft rejection and ageing. The trend in group E was relatively higher than that in group B, with cyclic fluctuation, but the difference was not statistically significant.

In vivo monitoring of ovarian graft bioluminescence revealed isograft survival for as long as 56 days in groups A, B and control group E. However, the photon quantity was much higher in groups B and E (Fig. 1A). Groups A,

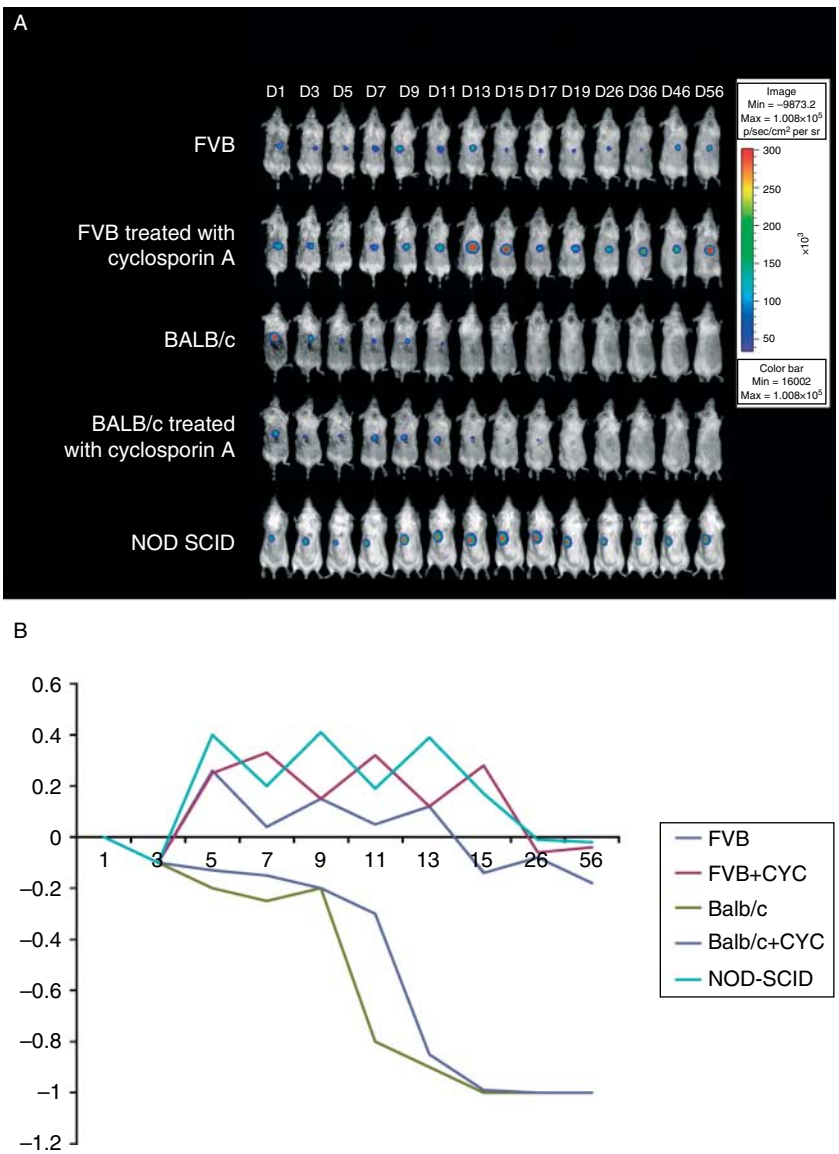

Figure 1 (A) Typical pattern of the representative engraftment of a mouse ovarian iso/allograft in each individual of each subgroup using *in vivo* BLI. The early loss of BLI indicated acute rejection at day 15 in group B and day 19 in group C. Longer survival of the graft, for up to 56 days after transplantation, in groups A, B and E indicated a lower rejection effect. (B) Typical trend in the photon quantity from the ovarian iso/allograft in each subgroup over time.

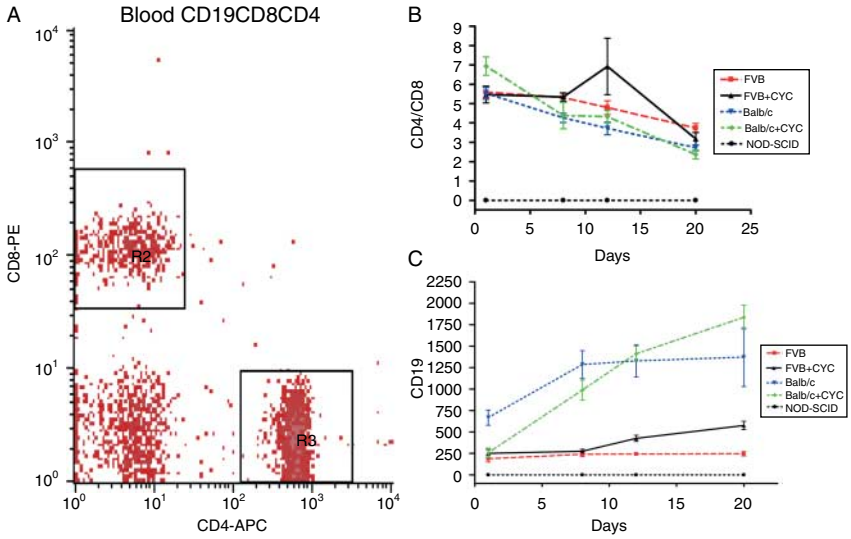

Figure 2 (A) Flow cytometric analysis of ($CD19^+$ positive) B-cells and subpopulations of T-cells, including $CD8^+/CD4^+$-positive cells, in the peripheral blood. (B) Peripheral T-cell subpopulations, monitored over time, revealed acute rejection accompanied by decreasing $CD4^+/CD8^+$ ratios and significant declines in groups C and D (allografts) compared with those in groups A and B (isografts; $P<0.0001$), with the development of acute rejection in the third week. Peripheral CD19 increased following acute rejection, and was significantly higher between day 1 and day 20 in groups C and D than in groups A and B ($P<0.001$). NOD–SCID mice lacking T- and B-cells were used as the control.

B and E showed fluctuating patterns of BLI engraftment with the oestrus cycle and follicle development as assayed by vaginal cytology and histology respectively (Fig. 1B). A complete loss of bioluminescence was noted on day 17 in group C (without cyclosporine A (CsA) treatment) and day 19 in group D (with CsA treatment). Similar to the BLI changes reflecting this engraftment pattern, histological analysis revealed extensive fat necrosis, myxoid degeneration and fibrosis, with no follicle presence, in groups C and D on day 19.

Peripheral T-cell subpopulations, examined across time, revealed lower $CD4^+/CD8^+$ ratios and significant declines in groups C and D (allografts) compared with those in groups A and B (isografts; $P<0.0001$; Fig. 2A and B), indicating the development of acute rejection throughout the third week in the allografts. Peripheral CD19 increased, and was significantly higher between day 1 and 20 in groups C and D than in groups A and B ($P<0.001$; Fig. 2A and C). Statistically significant differences were observed in the $CD4^+/CD8^+$ ratios and CD19 expression between the four experimental groups and the control group lacking T- and B-cells.

Immunohistochemical analysis of $CD4^+/CD8^+$ cells in the ovarian graft showed weak and no staining in groups A and B respectively from day 1. $CD4^+/CD8^+$ cell infiltration of the ovarian graft produced mild staining on day 1 in group C but strong staining on days 8, 12 and 20 after transplantation in groups C and D (Fig. 3A–F, Table 1). Group E was always used as the control, with no $CD4^+/CD8^+$ cell infiltration.

Consistent with the fluctuations in BLI, the ovarian follicles remained in groups A, B and E on day 56 but had vanished by day 19 because of fat necrosis in the grafts in groups C and D. Hormone activity revealed the presence of all four stages of the oestrus cycle, which is consistent with follicular development, in groups A, B and E. Compared with the fresh ovarian fragment and control group E, which showed various stages of follicular development, group E showed significantly lower numbers of follicles than the fresh control on day 0 but statistically more than groups A and B, and the primordial follicle count was higher in group B than in group A 56 days after transplantation (Fig. 4A–C and Table 2). Generalized myxoid degeneration and fat

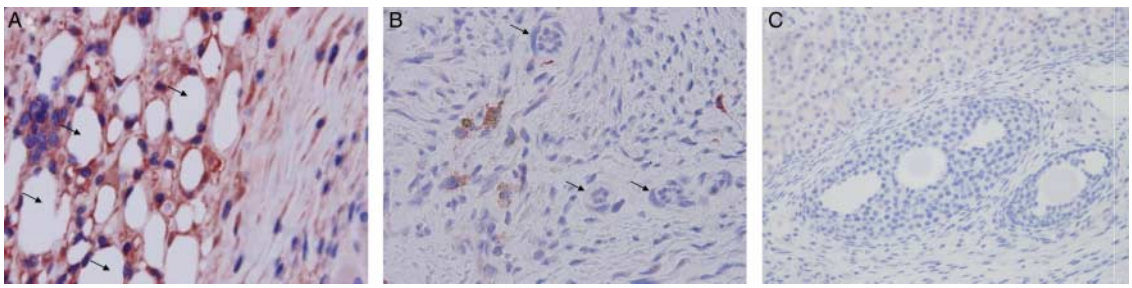

Figure 3 Immunohistochemical staining demonstrated $CD8^+/CD4^+$-positive cells infiltrating the mouse ovarian graft. (A) Semiquantitatively graded strong staining for $CD8^+$-positive (×1000) and $CD4^+$-positive (×1000) cells and fat necrosis (arrowhead) in the allograft in Balb/c wild-type mice on day 6. (B) Semiquantitatively graded weak staining for $CD8^+$-positive (×1000) and $CD4^+$-positive (×1000) cells and primordial follicles (arrowhead) in an isograft in an FVB/N wild-type mouse treated with cyclosporin A on day 6. (C) Non-immunohistochemical staining for $CD4^+/CD8^+$ (×400) cells in NOD–SCID mice.

Table 1 Profile of immunohistochemical staining for infiltrating $CD4^+/CD8^+$-positive cells in ovarian grafts over time.

Group	T-cell	D1	D8	D12	D20
FVB	CD4/CD8	+/+	+/+	+/+	+/+
FVB+CYC	CD4/CD8	−/−	−/−	−/−	−/−
Balb/c	CD4/CD8	+~++/+~++	++/++	++/++	++/++
Balb/c+CYC	CD4/CD8	+/+	++/++	++/++	++/++
NOD–SCID	CD4/CD8	−/−	−/−	−/−	−/−

(++), strong stain; (+), weak stain; (−), no stain.

necrosis were observed, without any follicles, in groups C and D 19 days after transplantation. However, only the dioestrus stage was completed after transplantation in groups C and D.

Discussion

With the application of fertility preservation, reproductive endocrine glands may resume their function without hormone replacement therapy, and females may regain their fertility after adequate gonad preservation or donation. The orthotopic ovarian allotransplantation used for Turner's syndrome restores the development of secondary sexual characteristics and menstruation, which echoes a series of ovarian isotransplantations in monozygotic twins (Mhatre *et al*. 2005, Silber *et al*. 2005, 2008, Silber & Gosden 2007). Regardless of the ethical issues, effective chronic immunosuppressant treatment warrants further study in this animal model. Fertility is an important criterion by which women are judged, and ovarian transplant technology has the potential to reduce culturally entrenched discrimination against infertile women (R Nidamboor, February 2003, Science in Africa, www.scienceinafrica.co.za/2003/february/ovary.htm).

In contrast to ovarian isografts, which constitute a minority of ovarian grafts, ovarian allografts can be used in a wide range of patients with gonad failure, including gonadal dysgenesis, POF, surgical castration and chemotherapy/radiation-induced damage. The success of allotransplantation depends on rejection immunology, which varies with tissue differences, human leukocyte antigen (HLA) typing and immunosuppressants (Sayegh & Turka 1998, Cjte *et al*. 2001, Pidwell & Burns 2007). If all other factors are optimal, such as donor management, functional state of the donor ovary, surgical procedures and intraoperative recipient management, the main cause of transplant failure is rejection.

Ovarian graft size and longevity have never been quantified *in vivo* in the same individuals. This *in vivo* monitoring model is the first model used to investigate ovarian iso- and allografts systemically and longitudinally using a real-time optical imaging.

BLI has become an important component of biomedical research. It is ideal for small animal models because it can monitor biological processes with great sensitivity, efficiency, economy and versatility (Zinn *et al*. 2008). The advantages of *in vivo* imaging over *in vitro* imaging include its high throughput, lack of radiation, easy operation, functional analysis, constant monitoring,

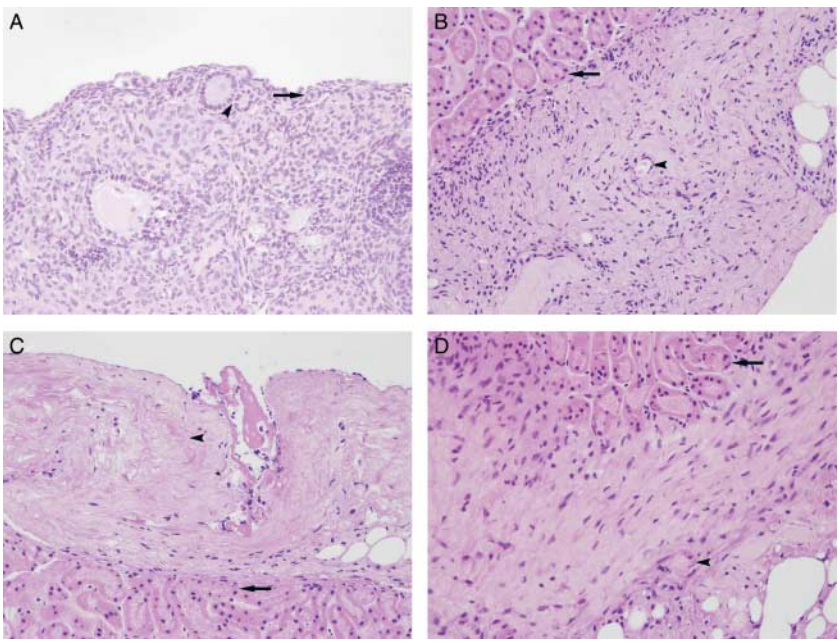

Figure 4 (A) Fresh control ovarian primordial follicles (arrow) and primary follicles (arrowhead; magnification, ×400). (B) Ovarian primordial follicles in group A (arrowhead) and renal tubules (arrow; magnification, ×400) 56 days after transplantation. (C) Ovarian primordial follicles in group B (arrowhead) and renal tubules (arrow; magnification, ×400) 56 days after transplantation. (D) Typical pattern of generalized myxoid degeneration, with no follicles (magnification, ×400) in groups C and D 20 days after transplantation.

Table 2 Comparison of primordial follicle counts in the control and experimental groups (on day 56 after the ovarian isografts and on day 20 after the ovarian allografts). Values are mean±S.D.

	Fresh	FVB	FVB+CYC	Balb/c	Balb/c+CYC	NOD–SCID
Day	0	56	56	20	20	56
Primordial follicles	130±15*	5±1.5*,†,‡,§	20±4.5*,†,‡	0*,†,‡,§	0*,†,‡,§	36±2.3*,†

*,†,‡,§Values sharing common superscripts in the same row differ significantly ($P<0.05$).

low variation, 3Rs (replacement, reduction and refinement), time efficiency through real-time imaging, digital quantum quantity in as little as 10 min by one researcher and the sacrifice of fewer mice.

In this study, we used transgenic donor mice carrying only a 712-bp luciferase transgene as the reporter, to create a significant genetically identical and non-identical model. The imaging technology has advanced to the point where it can rapidly reveal the fates of ovarian grafts, which have previously been elusive.

The different recipient strains had the same haplotype as the FVB wild-type recipients or a different haplotype (Balb/C, allotransplantation) from that of the transgenic donor strain (FVB strain). Routine HLA typing for solid organ transplantation in humans has been concerned with the prognosis of chronic rejection. Therefore, we also used CsA, the most commonly used immunosuppressant, to test its suppression of ovarian rejection in this model (Sheldon & Poulton 2006).

Ovaries are not immunologically privileged. It is reasonable to use more aggressive and multiple chronic immunotherapies for allografts (Parkmann 1988, Paul 2001). The transplanted ovarian tissue represents a continuous source of HLA alloantigens capable of inducing a rejection response at any time after transplantation. Because this cannot be eliminated, the allograft continuously activates the T- and B-cell immune system, resulting in the lifelong overproduction of cytokines, constant cytotoxic activity and sustained alteration of the graft vasculature (Bellanti & Kadlec 1985, Bellanti & Rocklin 1985, McDevitt 1985, Roitt *et al*. 1985, Sompayrac 1999). The ovarian isografts, with or without CsA treatment, showed reasonably longer survival for up to 56 days with *in vivo* monitoring. CsA treatment alone was not effective against the rejection of ovarian allografts, which showed a limited longevity of 20 days.

Bioluminescence showed the complete rejection of allografts, with or without CsA, in 20 days. The absence of an oestrus cycle indicated the early loss of function. Ovarian isografts survived functionally for more than 56 days, but stronger luminescence also indicated a better outcome after CsA treatment. This study is consistent with previous reports that showed allografts, in contrast to isografts, were completely rejected in 20 days (Gosden 2007).

Allogeneic ovarian transplantation is not immunoprivileged, and will not succeed unless the recipient immune system is down-regulated. Furthermore, this downregulation by immunomodulation must be maintained on a lifelong basis because antigens (the allograft) are not self-limiting in solid organ transplantation, but are always present. The continued introduction of new immunosuppressants will provide greater access to transplantation (Bellanti & Kadlec 1985, Bellanti & Rocklin 1985, McDevitt 1985, Roitt *et al*. 1985, Sompayrac 1999).

Non-obese diabetic (NOD)–severe combined immunodeficient (SCID) mice, used as the control group for long-surviving ovarian grafts, are deficient in B-cell and T-cell functions, and lack detectable B-cells and pre-B-cells. However, they have normal numbers of natural killer cells, the main effectors of non-major histocompatibility complex-restricted immunity, which also includes the recognition of haemopoietic histocompatibility antigens on bone marrow allografts. Immune responses other than those involving T-cells and B-cells warrant further study.

In conclusion, transplantation models using luciferase-based imaging have revealed that *in vivo* monitoring with BLI of an ovarian transplant can detect changes in the functional mass resulting from immunological events, which ultimately affect the quality of the graft function and could potentially be used to test new immunosuppressants.

Materials and Methods

Care and use of animals

The 8-week-old FVB/N-Tg(*RNA polymerase II (PolII)–Luc*)Ltc transgenic donor mouse, H-2 haplotype (H^q_2), was created using the transgenic services of Level Biotechnology Inc., Hsi-Chih City, Taiwan (Fig. 5A). The construct (gene fragment) *PolII–Luc* contains the 712-bp mouse *PolII* promoter and a modified firefly luciferase cDNA (Promega pGL-2; Fig. 5B and C). This transgenic line was created using pronuclear microinjection of the *PolII–Luc* transgene into fertilized FVB/N embryos at the Level Transgenic Center. Transgenic founder cells expressing the transgene were analysed for their expression patterns and tested for their germline transmission (Fig. 5C). The transgenic line was maintained as hemizygotes. An inbred strain of 8-week-old FVB/NJNarl wild-type mice with the H-2 haplotype (H^q_2) and 8-week-old Balb/cByJNarl wild-type mice with the H-2 haplotype (H^d_2) was obtained from the National Laboratory Animal Center, Taiwan, ROC. Another control recipient 8-week-old Fox Chase female NOD mice–SCID mice (C.B-17 SCID) were obtained from BioLASCO, Taipei, Taiwan.

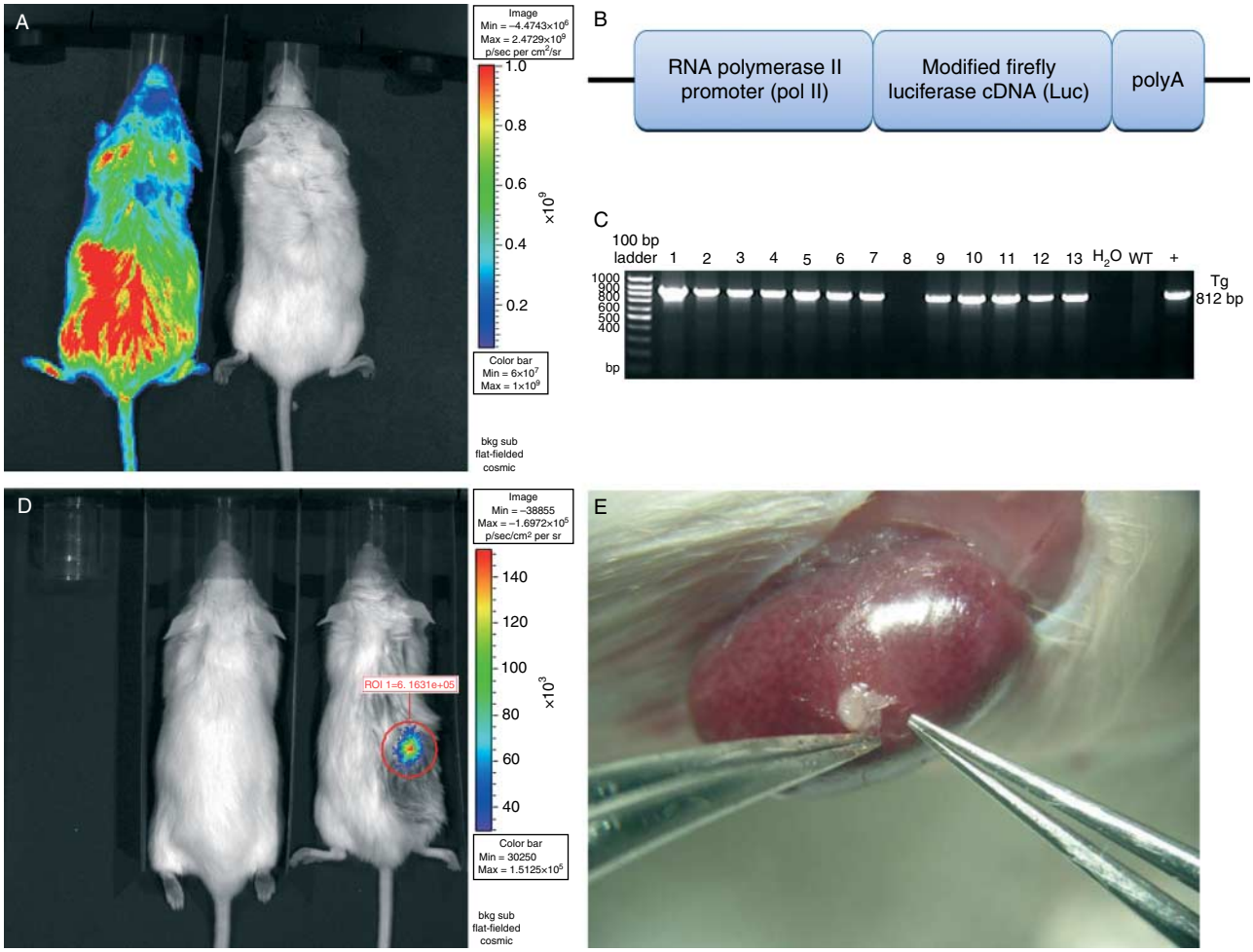

Figure 5 FVB/N-Tg(*PolII–Luc*)Ltc transgenic mice. (A) Before (right) and after (left) treatment with luciferin; the light emitted by the transgene reaction was detected with the IVIS Imaging System. Luciferase expression was detectable in all organs of the transgenic mouse. (B) Schematic representation of the transgenic construct containing the 712-bp mouse RNA polymerase II (*PolII*) promoter and a modified firefly luciferase cDNA (Promega pGL-2). (C) Genotyping the transgene by PCR. (D) FVB/N-Tg(*PolII–Luc*)Ltc as the donor mouse (left) and no *in vivo* bioluminescence in the FVB/N wild-type recipient mouse (right). Transplanted ovarian tissue of the transgenic FVB/N-Tg(PolII–Luc)Ltc mouse after i.p. luciferin treatment, with quantification of the quantum bioluminescent imaging data. (E) Surgical techniques used for ovarian transplantation from the transgenic FVB/N-Tg(*PolII–Luc*)Ltc mouse to the sub-renal capsule of the recipient mouse.

All the mice were housed under a 12 h light:12 h darkness regime at 22–24 °C, with food and water supplied without restriction. All procedures described here were reviewed and approved by the Animal Experimental Committee at the National Defense Medical Center and Tri-Service General Hospital, Taipei, Taiwan, ROC, in accordance with the Guiding Principles for the Care and Use of Laboratory Animals.

Operative designs

The mice were treated with ketamine (50 mg/kg) and xylazine (15 mg/kg) given i.p. to induce general anaesthesia. Donor mice (8 weeks old, sexually mature) and recipient mice (8 weeks old, sexually mature) underwent bilateral ovariectomy 1 week before transplantation. The recipient mice included group A ($n=5$, FVB/N wild-type mice with the H-2 haplotype [H_2^q] (isogenic) without daily CsA treatment); group B ($n=5$, FVB/N wild-type mice with the H-2 haplotype [H_2^q] with daily 25 mg/kg CsA treatment); group C ($n=5$, Balb/c wild-type mice with the H-2 haplotype [H_2^d] (allogeneic) without daily CsA treatment); group D ($n=5$, Balb/c wild-type mice with the H-2 haplotype [H_2^d] with 25 mg/kg CsA treatment); and group E ($n=5$, NOD–SCID mice). The donor ovaries were divided into several fragments, followed by transplantation into the unilateral sub-renal capsule of each recipient strain (Fig. 5E). The mice in groups B and D were given CsA (25 mg/kg per day i.p.), starting 1 day before transplantation until they were killed. Another paired recipient group was processed under the same conditions for *in vitro* immunohistochemistry.

In vivo *BLI* (in vivo *tracking of viable cells and tissue*)

The mice were anaesthetized before injection with luciferin, and the transgene expression was measured (Fig. 5A). Reporter genes can be used to assay the activity of a particular *PolII* promoter in each viable cell. The reporter gene product is the

luciferase enzyme. Luciferase catalyses a reaction with luciferin, producing light. The reporter gene is simply placed under the control of the target promoter (*PolII*), and the activity of the reporter gene product is measured. Luciferin (Xenogen Corporation, Caliper Life Science, Alameda, CA, USA; catalogue #XR-1001) was prepared freshly in PBS (15 mg/ml) and sterilized by filtration. FVB/N-Tg(*PolII–Luc*)Ltc animals were injected i.p. with luciferin (150 mg/kg) 10 min before imaging, anaesthetized (1–3% isoflurane) and placed in a lightproof camera box. The mice were imaged dorsally for 3 min at high-resolution settings with a field of view of 20 cm. The light emitted from the transgene was detected with the IVIS Imaging System 50 Series (Caliper Life Science), digitized and displayed on a monitor. Living Image software (Caliper Life Science) takes data from the camera and displays the information on a pseudocolour scale, with colours representing the variations in signal intensity. The signals were quantified and archived using the Living Image software. Photons from the kidneys were quantified from the dorsal images using oval regions of interest (ROIs) of 3.5×3.5 cm^2 centred over the kidneys (Fig. 5D). The absolute intensity calibration of the IVIS Imaging System 50 Series was accomplished with a calibrated eight-inch integrating sphere (OL Series 425 Variable Low-Light-Level Calibration Standard, Optronic Laboratories, Inc., Orlando, FL, USA). We measured the ROI by imaging the counts detected by the CCD camera digitizer on the integrating sphere, which were converted to physical units of radiance in photons/s per cm^2 per steradian (Rice *et al.* 2006). Background signals were evaluated daily, and background subtraction calculations were performed with the Living Image software.

Subpopulations of CD4$^+$/CD8$^+$-positive T-cells and CD19$^+$-positive B-cells in mouse blood detected by flow cytometry

Peripheral blood cells were collected and stained with phycoerythrin-conjugated anti-mouse CD8 antibody (Ab), allophycocyanin-conjugated anti-mouse CD4 Ab, and FITC-conjugated anti-mouse CD19 Ab (BD Bioscience Pharmingen, San Jose, CA, USA; Riccardo *et al.* 2005). The cells were detected with flow cytometry on days 1, 5, 12 and 20 after ovarian graft transplantation.

Immunohistochemistry of CD4$^+$/CD8$^+$ cells in the ovarian graft

MABs labelled by the streptavidin–biotin (LSAB2; Dako Corporation, Santa Barbara, CA, USA) method were used for immunohistochemistry. The antibodies used were directed against CD4 (NeoMarkers, Fremont, CA, USA) and CD8 (CD4 Ab8, CD8 Ab1; NeoMarkers; Sato *et al.* 2005). Each Ab was tested on ten pairs of sections, and the staining was scored as negative, weak or strong, according to the staining intensity. The intensity scores were graded from − to ++(−, none; +, weak and ++, strong staining).

Detection of oestrus cycle

Vaginal smears from the mature virgin female wild-type recipient mice (8 weeks old) were collected twice daily. The normal oestrus cycle of a laboratory mouse is 4–6 days in length, and has four stages: pro-oestrus, oestrus, metoestrus and dioestrus (Kimmin *et al.* 2004, Staley & Scharfman 2005). Cycle length was determined as the length of time between two consecutive occurrences of oestrus in animals that had progressed through at least three consecutive oestrous cycles. A 12 h light:12 h darkness cycle was maintained automatically, with lighting changes occurring at 0600 and 1800 h.

Ovarian follicles

Ovarian cortex biopsies involved cutting the samples into 5-μm sections, fixing them in 10% formalin, and staining them with hematoxylin and eosin in paraffin sections to examine the various stages of follicular development. The primordial follicle count was measured in ten consecutive sections.

Statistical analysis

Light was quantified in terms of the proportional change from baseline (day 1). The peripheral T-cell subpopulation and B-cell activation were also assayed over time. To test the statistical significance of differences, ANOVA was used at each time point, with multiple comparisons adjusted using the Scheffe method. All analyses were performed with SAS 8.0, and $P<0.05$ was considered significant.

Declaration of interest

The authors declare that there is no conflict of interest that could be perceived as prejudicing the impartiality of the research reported.

Funding

The work was supported in part by NSC-96-2314-B-016-023, a grant from National Science Council, Taiwan, ROC and in part by TSGH-C97-65 and TSGH-C96-47, the grants of Tri-Service General Hospital, Taiwan, ROC.

Acknowledgements

The authors wish to thank Dr Hong-Wei Gao and Dr Chih-Kung Lin of the Tri-Service General Hospital (Taipei, Taiwan, ROC) for their assistance for immunohistochemistry, and Wei-Jen Shang for his technique for bioluminescence imaging.

References

Bellanti JA & Kadlec JV 1985 General immunology. In *Immunology III*, pp 16–53. Ed. JA Bellanti. Philadelphia, PA: WB Saunders Co.

Bellanti JA & Rocklin RE 1985 Cell-mediated immune function. In *Immunology III*, pp 176–188. Ed. JA Bellanti. Philadelphia, PA: WB Saunders Co.

Chen SU, Lien YR, Chao KH, Ho HN, Yang YS & Lee TY 2003 Effects of cryopreservation on meiotic spindles of oocytes and its dynamics after thawing: clinical implications in oocyte freezing – a review article. *Molecular and Cellular Endocrinology* **28** 101–107.

Cjte I, Rogers NJ & Lechler RI 2001 Allorecognition. *Transfusion Clinique et Biologique* **8** 318–323.

Donnez J, Martinez-Madrid B, Jadoul P, Van Langedonckt A, Demylle D & Dolmans MM 2006 Ovarian tissue cryopreservation and transplantation: a review. *Human Reproduction Update* **12** 519–535.

Fowler M, Virostko J, Chen Z, Poffenberger G, Radhika A, Brissova M, Shiota M, Nicholson Wendell E, Shi Y, Hirshberg B *et al.* 2005 Assessment of pancreatic islet mass after islet transplantation using *in vivo* bioluminescence imaging. *Transplantation* **79** 768–776.

Gosden RG 2007 Survival of ovarian allografts in an experimental animal model. *Pediatric Transplantation* **11** 628–633.

Hoshinaga K, Mohanakumar T, Goldman MH, Wolfgang TC, Szentpetery S, Lee HM & Lower RR 1984 Clinical significance of *in situ* detection of T lymphocyte subsets and monocyte/macrophage lineages in heart allografts. *Transplantation* **38** 634–637.

Ibrahim S, Dawson DV, Van Trigt P & Sanfilippo F 1993 Differential infiltration by CD45RO and CD45RA subsets of T cells associated with human heart allograft rejection. *American Journal of Pathology* **142** 1794–1803.

Kim SS, Battaglia DE & Soules MR 2001 The future of human ovarian cryopreservation and transplantation: fertility and beyond. *Fertility and Sterility* **75** 1049–1056.

Kimmin S, Lim HC & MacLaren LA 2004 Immunohistochemical localization of integrin alpha V beta 3 and osteopontin suggests that they do not interact during embryo implantation in ruminants. *Reproductive Biology and Endocrinology* **2** 19.

Kuwayama M, Vajta G, Kato O & Leibo SP 2005 Highly efficient vitrification method for cryopreservation of human oocytes. *Reproductive Biomedicine Online* **11** 300–308.

McDevitt HO 1985 The HLA system and its relation to disease. *Hospital Practice* **20** 57–72.

Mhatre P, Mhatre J & Magotra R 2005 Ovarian transplant: a new frontier. *Transplantation Proceedings* **37** 1396–1398.

Min JJ, Ahn Y, Moon S, Kim YS, Park JE, Kim SM, Le UN, Wu JC, Joo SY, Hong MH *et al.* 2006 *In vivo* bioluminescence imaging of cord blood derived mesenchymal stem cell transplantation into rat myocardium. *Annals of Nuclear Medicine* **20** 165–170.

Parkmann R 1988 Cyclosporine: graft versus host disease and beyond. *New England Journal of Medicine* **319** 110–111.

Paul LC 2001 Immunologic risk factors for chronic allograft dysfunction. *Transplantation* **71** SS17–SS23.

Pidwell DJ & Burns C 2007 The immunology of composite tissue transplantation. *Clinics in Plastic Surgery* **34** 303–317.

Riccardo S, Gian LM, Alessandra S, Alberto B, Paolo B, Pao DB, Amedea D, Massimo F, Angelo G, Francesca G *et al.* 2005 Autologous HSCT for severe progressive multiple sclerosis in a multicenter trial: impact on disease. *Blood* **105** 2601–2607.

Rice BW, Cable MD & Nelson MB 2006 *In vivo* imaging of light-emitting probes. *Journal of Biomedical Optics* **6** 432.

Roitt I, Brostoff J & Male D 1985 Major histo-compatibility complex. In *Immunology,* pp 4.1–4.12. Eds I Roitt, J Brostoff & D Male. St Louis, MO: The CV Mosby Co.

Sato E, Olson SH, Ahn J, Bundy B, Nishikawa H, Qi F, Jungbluth AA, Frosina D, Gnjatic S, Ambrosone C *et al.* 2005 Intraepithelial $CD8^+$ tumor-infiltrating lymphocytes and a high $CD8^+$/regulatory T cell ratio are associated with favorable prognosis in ovarian cancer. *PNAS* **102** 18538–18543.

Sayegh MH & Turka LA 1998 The role of T-cell costimulatory activation pathways in transplant rejection. *New England Journal of Medicine* **338** 1813–1821.

Sheldon S & Poulton K 2006 HLA typing and its influence on organ transplantation. *Methods in Molecular Biology* **333** 157–174.

Silber SJ & Gosden RG 2007 Ovarian transplantation in a series of monozygotic twins discordant for ovarian failure. *New England Journal of Medicine* **356** 1382–1384.

Silber SJ, Lenahan KM, Levine DJ, Pineda JA, Gorman KS, Friez MJ, Crawford EC & Gosden RG 2005 Ovarian transplantation between monozygotic twins discordant for premature ovarian failure. *New England Journal of Medicine* **353** 58–63.

Silber SJ, DeRosa M, Pineda J, Lenahan K, Grenia D, Gorman K & Gosden RG 2008 A series of monozygotic twins discordant for ovarian failure: ovary transplantation (cortical versus microvascular) and cryopreservation. *Human Reproduction* **23** 1531–1537.

Sompayrac L 1999 *How the Immune System Works*. Malden, MA: Blackwell Science, Inc.

Staley K & Scharfman H 2005 A woman's prerogative. *Nature Neuroscience* **8** 697–699.

Woodruff MFA 1960 *The Transplantation of Tissues and Organs*. Springfield, IL: Charles C Thomas.

Yang YL, Dou KF & Li KZ 2003 Influence of intrauterine injection of rat fetal hepatocytes on rejection of rat liver transplantation. *World Journal of Gastroenterology* **9** 137–140.

Yazawa N, Hamaguchi Y, Poe JC & Tedder TF 2005 Immunotherapy using unconjugated CD19 monoclonal antibodies in animal models for B lymphocyte malignancies and autoimmune disease. *PNAS* **102** 15178–15183.

Zinn KR, Chaudhuri TR, Szafran AA, O'Quinn D, Weaver C, Dugger K, Lamar D, Kesterson RA, Wang X & Frank SJ 2008 Noninvasive bioluminescence imaging in small animals. *ILAR Journal* **49** 103–115.

Received 10 October 2009
First decision 6 November 2009
Revised manuscript received 23 March 2010
Accepted 27 April 2010